PHYSICAL REVIEW E VOLUME 58, NUMBER 1 JULY 1998

Weakly nematic–highly nematic phase transitions in main-chain liquid-crystalline polymers

Akihiko Matsuyama* and Tadaya Kato
Department of Chemistry for Materials, Faculty of Engineering, Mie University, Tsu Mie 514, Japan

(Received 16 December 1997; revised manuscript received 12 February 1998)

A mean field theory is introduced to describe the nematic-isotropic phase transitions (NIT) of main-chain liquid-crystalline polymers (MLCPs) which consist of rigid mesogens and spacers with various degrees of flexibility. We here assume that two neighboring bonds on the spacers have either bent or straightened conformations and the straightened conformation gives rise to a rigid rodlike shape. The theory takes into account not only the nematic ordering of mesogens but also the partial ordering of spacer segments in the nematic phase. On the basis of the Onsager type excluded volume interactions and the Maier-Saupe model for orientational-dependent attractive interactions between rigid segments, we derive the free energy of the MLCPs in melts. The NIT temperature, the order parameter of mesogens, and that of spacers are examined as a function of the spacer length, the flexibility of spacers, and the strength of the anisotropic interactions. We also derive the Landau–de Gennes expansion of our free energy. We find that the NIT temperature T_{NI} of a MLCP with semiflexible spacers has a minimum as a function of the spacer length n_s. At small values of n_s, we have a weakly nematic phase which is mostly formed by the ordering of the mesogens and the spacers play a softening role. At large values of n_s, we have a highly nematic phase where the straightened segments on the spacers and the mesogens are highly ordered and the spacers play a stiffening role. The two different nematic phases are discussed in the phase diagrams of the temperature-spacer length plane. [S1063-651X(98)03007-4]

PACS number(s): 61.30.Cz, 64.70.Md, 61.82.Pv

I. INTRODUCTION

Thermotropic liquid-crystalline polymers have been investigated as new materials with remarkable mechanical, optical, and electrical properties. Main-chain liquid-crystalline polymers (MLCPs) consist of rigid mesogens connected by spacers with various degrees of flexibility, such as methylene and ethylene glycol groups. The flexibility of the MLCP can be regulated by using different chemical structures or different length of the mesogens and spacers. The performances of the MLCP and the nematic-isotropic phase transition (NIT) are closely related to these molecular parameters [1–3].

Some experimental studies have suggested that the spacers play an important role in determining the degree of organization in a liquid-crystalline mesophase [4–10]. NMR studies on copolyesters (4,4′-dihydroxy, α, α'-dimethylbenzalazine) over a wide temperature range have addressed the existence of strong correlations between the mesogens and spacers in the nematic phase [7,9]. Then the accounting for the partial ordering of spacers in the nematic phase is necessary in the theoretical treatment of MLCP systems.

Liquid crystals of low molecular weight are modeled by rigid rodlike molecules interacting with each other through the hard-core repulsions [11] and the attractive intermolecular interactions [12,13]. The problems of the liquid crystallinity in the systems containing liquid-crystalline polymers are treated by several theoretical models such as lattice models [14–19], elastic wormlike chain models [20–27], freely jointed models [28], and persistent chains [29]. These theories, however, cannot describe the orientational ordering of spacers in a nematic phase because the model polymers consist of homogeneous chains. In order to describe the MLCPs with flexible and rigid segments, we must consider that the two constituent monomers differ in flexibility [30–34]. Some years ago, based on the Matheson-Flory theory for MLCPs [19], Vasilenko *et al.* [30] calculated the free energy of MLCPs, in which they take into account the partial ordering of flexible spacers and focused on the NIT in athermal melts. Wang and Warner [32] presented a molecular model to describe nonhomogeneous MLCPs, in which the MLCP is composed in sequence of rigid rodlike mesogen units and spacers denoted by a wormlike model. A lattice theory proposed by Flory [14] has considered the isotropic solution of semiflexible polymer chains in which two neighboring bonds on the chain have either bent or straightened conformations. To describe the NIT of the semiflexible polymers, we recently presented a simple mean field model combining the Flory theory with the Maier-Saupe model for the orientation-dependent attractive interactions between straightened bonds [35].

In this paper we extend the previous model [35] to the melts of MLCPs, which consist of rigid mesogens and spacers with various degrees of flexibility. We here assume that the two neighboring bonds on the spacers have either bent or straightened conformations and the straightened conformation gives rise to a rigid rodlike shape. The theory takes into account both the nematic ordering of mesogens and the partial ordering of spacer segments in the nematic phase. On the basis of the Onsager theory for hard-core repulsive interactions [11] and the Maier-Saupe model for orientational-dependent attractive interactions [12,13] between straightened segments, we derive the free energy of the MLCPs in melts. The nematic-isotropic transitions, the order parameter of mesogens, and that of spacers are examined as a function of the spacer length, the flexibility of spacers, and the strength of the anisotropic interactions. We also derive the Landau–de Gennes expansion of our free energy.

---

*Author to whom correspondence should be addressed.

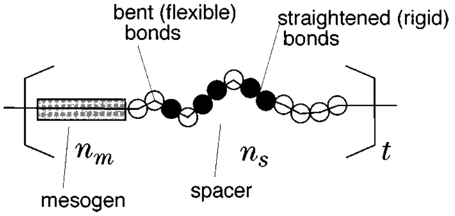

FIG. 1. Model of a main-chain liquid-crystalline polymer (MLCP). The repeating unit in the MLCP consists of rigid-mesogenic groups whose axial ratio is n_m and spacer groups containing n_s segments. The total number of segments on the MLCP is $n=(n_m+n_s)t$, where t is the number of repeating units. The symbols ● and ○ show the segments on the straightened and bent bonds on the spacers, respectively.

The paper is organized as follows. We first describe the free energy of MLCPs in melts, in which we take into account the three physical parameters; the fraction of straightened segments on the spacers, the orientational order parameter of mesogens, and that of spacers. In Sec. III, by minimizing the free energy, we obtain the values of these three parameters in thermal equilibrium conditions. In Sec. IV we show the detailed numerical results. In the Appendix, Landau–de Gennes expansion of our free energy is derived and the approximate formulas for the NIT temperature and the order parameter are given as a function of spacer length, the flexibility of spacers, and temperature.

II. FREE ENERGY FOR MELTS OF MAIN-CHAIN LIQUID-CRYSTALLINE POLYMERS

We consider a melt of a main-chain liquid-crystalline polymer. The repeating units in the MLCP consist of a rigid-mesogenic unit with axial ratio n_m and spacer units which have the number n_s of segments. The total number of segments on the MLCP is $n=(n_m+n_s)t$, where t is the number of repeating units. (See Fig. 1.) In order to take into account the partial orientational ordering of spacers in a nematic phase, we here assume that the two neighboring bonds on the spacers have either bent or straightened conformations and the conformational free energy of the straightened bond is $|\epsilon_0|$ less than that of the bent bonds. For example, the energy difference between the trans and the gauch state of C—C bonds on n-alkanes gives values of the order of the thermal energy [36] and so the straightened state of the bonds is energetically favored (however, it is entropically unfavorable). To describe the nematic-isotropic phase transition in the MLCP, we here assume that the straightened conformation gives rise to a rigid rodlike shape. Then the orientational ordering (nematic behavior) of the straightened bonds on the spacers as well as the rigid mesogens can be induced by both the excluded volume interactions and the orientational-dependent attractive interactions. Hereafter we call the segments in straightened bonds and that in bent bonds ‘‘rigid’’ and ‘‘flexible’’ segments, respectively.

The free energy of the MLCP in melts can be given by

$$F=F_{\mathrm{bent}}+F_{\mathrm{nem}}. \tag{2.1}$$

The first term F_{bent} shows the free energy change needed to straighten bent bonds on the spacers. In our systems, F_{bent} is given by

$$\beta F_{\mathrm{bent}}=n_r t(\beta f_0)-S_{\mathrm{comb}}/k_B-\Delta S_{\mathrm{conf}}/k_B, \tag{2.2}$$

where $\beta\equiv 1/k_B T$, T is the absolute temperature, k_B is the Boltzmann constant, f_0 is the local free energy change needed to straighten a bent bond, and n_r shows the number of rigid segments on spacers. The second term in Eq. (2.2) is the combinatorial entropy related to the number of ways to select n_r segments out of the number n_s of the spacer segments and is given by

$$S_{\mathrm{comb}}/k_B=t\ \ln\frac{n_s!}{n_r!(n_s-n_r)!}. \tag{2.3}$$

By using Stirling's approximation, Eq. (2.3) can be rewritten as

$$S_{\mathrm{comb}}/k_B=-tn_s[x\ \ln x+(1-x)\ln(1-x)], \tag{2.4}$$

where

$$x\equiv n_r/n_s \tag{2.5}$$

shows the fraction of rigid (straightened) segments on the spacers. The third term in Eq. (2.2) shows the change in conformational entropy of chains. According to Flory's lattice theory, the conformational entropy $S_{\mathrm{conf}}[m]$ of a flexible chain with m flexible segments is given by [37]

$$S_{\mathrm{conf}}[m]/k_B=\ln\left[\frac{mz(z-1)^{m-2}}{\sigma\exp(m-1)}\right], \tag{2.6}$$

where z is the lattice coordination number and σ is the symmetry number of the chain. Equation (2.6) is the entropy gain to bring a chain from the hypothetical crystalline (straightened) state to a flexible amorphous state. When the n_r segments out of the n_s segments on a flexible spacer are replaced by rigid segments, we have the conformational entropy change ΔS_{conf} which is given by

$$\Delta S_{\mathrm{conf}}=S_{\mathrm{conf}}[(n_s-n_r)t]-S_{\mathrm{conf}}[n_s t]. \tag{2.7}$$

This entropy ΔS_{conf} was omitted in the earlier work [35]. Substituting Eq. (2.6) into Eq. (2.7) we obtain

$$\Delta S_{\mathrm{conf}}/k_B=-\ln\left[\frac{n_s}{n_s-n_r}\left(\frac{z-1}{e}\right)^{n_r t}\right]. \tag{2.8}$$

From Eqs. (2.4) and (2.8), the free energy (2.2) can be expressed as

$$\beta F_{\mathrm{bent}}=np\left[x\beta f_0+x\ln\left(\frac{z-1}{e}\right)-\frac{1}{n_s t}\ln(1-x)+x\ln x+(1-x)\ln(1-x)\right], \tag{2.9}$$

where

$$p\equiv n_s/(n_m+n_s)=n_s t/n \tag{2.10}$$

shows the fraction of the spacer segments on the repeating unit.

The second term F_{nem} in Eq. (2.1) shows the free energy for the nematic ordering. On the basis of the excluded volume interactions [11] and the orientational-dependent (Maier-Saupe) interactions [12,13], we consider three coupling terms of the anisotropic interactions. Let ν_{mm} be the orientational-dependent (Maier-Saupe) interactions between mesogen segments, ν_{ms} be that between a mesogen and a rigid segment on spacers, and ν_{ss} be that between rigid segments on spacers. The volume fraction g_r of the rigid segments on the spacer is given by

$$g_r = n_r t/n = xp. \tag{2.11}$$

On the basis of both the Maier-Saupe model and the Onsager theory, the free energy of the nematic ordering is given by [38]

$$\begin{aligned}\beta F_{\mathrm{nem}} = n\Bigg[& \frac{(1-p)}{n_m}\int f_m(\theta)\ln 4\pi f_m(\theta)\,d\Omega \\ & + \frac{px}{n_r}\int f_s(\theta)\ln 4\pi f_s(\theta)\,d\Omega - \frac{1}{2}\nu_{mm}S_m^2(1-p)^2 \\ & - \nu_{ms}S_mS_s(1-p)px - \frac{1}{2}\nu_{ss}S_s^2p^2x^2 \\ & + (\rho_{mm}-1)(1-p)^2 + 2(\rho_{ms}-1)(1-p)px \\ & + (\rho_{ss}-1)p^2x^2\Bigg],\end{aligned} \tag{2.12}$$

where $d\Omega \equiv 2\pi \sin\theta d\theta$, and θ is the angle between the rigid segments and the director of the orienting field. The $f_m(\theta)$ and $f_s(\theta)$ show the orientational distribution functions of the mesogen segments and that of the rigid segments on the spacers, respectively. The first two terms represent the decrease of entropy due to the nematic ordering of the mesogens and the rigid segments on the spacers. The orientational order parameter S_m of the mesogen segments is given by

$$S_m = \int P_2(\cos\theta) f_m(\theta)\,d\Omega, \tag{2.13}$$

and the orientational order parameter S_s of the rigid segments on the spacers is given by

$$S_s = \int P_2(\cos\theta) f_s(\theta)\,d\Omega, \tag{2.14}$$

where $P_2(\cos\theta) \equiv 3(\cos^2\theta - 1/3)/2$. The last three terms in Eq. (2.12) show the excluded volume interactions between rigid segments and the function $\rho_{ij}(i,j=m,s)$ is given by [11]

$$\rho_{ij} = \frac{4}{\pi}\int\int \sin\gamma(\theta,\theta') f_i(\theta) f_j(\theta')\,d\Omega\, d\Omega'. \tag{2.15}$$

In the isotropic phase, we have $f_i(\theta) = 1/(4\pi)$ and $\rho_{ij} = 1$.

III. NEMATIC ORDERING OF MESOGENS AND SPACERS

By minimizing the free energy (2.1), we can obtain the values of the order parameters S_m, S_s, and the fraction x in thermal equilibrium conditions.

The orientational distribution function $f_m(\theta)$ of the mesogen segments is determined by the free energy (2.12) with respect to this function: $[\partial F_{\mathrm{nem}}/\partial f_m(\theta)]_{x,f_s} = 0$. This leads to the integral equation

$$\begin{aligned}\ln 4\pi f_m(\theta) = {} & C_m + n_m[\nu_{mm}S_m(1-p) + \nu_{ms}S_spx]P_2(\cos\theta) \\ & - \frac{8}{\pi}n_m\Bigg[(1-p)\int \sin\gamma(\theta,\theta') f_m(\theta')\,d\Omega' \\ & + px\int \sin\gamma(\theta,\theta') f_s(\theta')\,d\Omega'\Bigg].\end{aligned} \tag{3.1}$$

Similarly, the distribution function $f_s(\theta)$ of the rigid segments on the spacers is determined by $[\partial F_{\mathrm{nem}}/\partial f_s(\theta)]_{x,f_m} = 0$. We then obtain

$$\begin{aligned}\ln 4\pi f_s(\theta) = {} & C_s + n_r[\nu_{ms}S_m(1-p) + \nu_{ss}S_spx]P_2(\cos\theta) \\ & - \frac{8}{\pi}n_r\Bigg[(1-p)\int \sin\gamma(\theta,\theta') f_m(\theta')\,d\Omega' \\ & + px\int \sin\gamma(\theta,\theta') f_s(\theta')\,d\Omega'\Bigg],\end{aligned} \tag{3.2}$$

where C_m and C_s are constants, which are determined by the normalization conditions

$$\int f_i(\theta)\,d\Omega = 1, \tag{3.3}$$

$i = m,s$. We here expand the kernel $\sin\gamma$ in Legendre polynomials:

$$\sin\gamma = \frac{\pi}{4} - \frac{5\pi}{32}P_2(\cos\theta)P_2(\cos\theta'). \tag{3.4}$$

Substituting Eq. (3.4) into Eqs. (3.1) and (3.2), we obtain the orientational distribution functions

$$f_m(\theta) = \frac{1}{Z_m}\exp[\eta_m P_2(\cos\theta)], \tag{3.5}$$

$$\eta_m \equiv n_m[(\nu_{mm} + \tfrac{5}{4})S_m(1-p) + (\nu_{ms} + \tfrac{5}{4})S_spx] \tag{3.6}$$

for the mesogen segments and

$$f_s(\theta) = \frac{1}{Z_s}\exp[\eta_s P_2(\cos\theta)], \tag{3.7}$$

$$\eta_s \equiv n_sx[(\nu_{ms} + \tfrac{5}{4})S_m(1-p) + (\nu_{ss} + \tfrac{5}{4})S_spx] \tag{3.8}$$

for the rigid segments on the spacers, where the constants $Z_i(i=m,s)$ are determined by the normalization condition (3.3). The terms ν_{ij} and 5/4 in Eqs. (3.6) and (3.8) correspond to the attractive and excluded volume interactions between rigid segments. From Eqs. (3.3), (3.5), and (3.7), the constant Z_i is given by

$$Z_m=2\pi I_0[\eta_m], \tag{3.9}$$

$$Z_s=2\pi I_0[\eta_s], \tag{3.10}$$

where the function $I_0[\eta_i]$ is defined as

$$I_q[\eta_i]\equiv\int_0^1[\tfrac{3}{2}(\cos^2\theta-\tfrac{1}{3})]^q\exp[\eta_i P_2(\cos\theta)]d(\cos\theta), \tag{3.11}$$

$q=0,1,2,\ldots.$ Substituting Eqs. (3.5) and (3.7) into Eqs. (2.13) and (2.14), we obtain two self-consistency equations for the two order parameters S_m and S_s:

$$S_m=I_1[\eta_m]/I_0[\eta_m], \tag{3.12}$$

$$S_s=I_1[\eta_s]/I_0[\eta_s], \tag{3.13}$$

and the average value of the order parameters is given by

$$S=S_m(1-p)+S_s px. \tag{3.14}$$

The function $\sigma_i\equiv\int f_i(\theta)\ln 4\pi f_i(\theta)d\Omega$ and ρ_{ij} in Eq. (2.12) are now given as a function of order parameters S_m and S_s as follows:

$$\sigma_i=\eta_i S_i-\ln I_0[\eta_i], \tag{3.15}$$

$$\rho_{ij}=1-\frac{5}{8}S_iS_j, \tag{3.16}$$

$i=m,s$. Substituting Eqs. (3.15) and (3.16) into Eq. (2.12), the free energy for the nematic ordering is given by

$$\beta F_{\mathrm{nem}}/n=\frac{1}{2}\left(\nu_{mm}+\frac{5}{4}\right)S_m^2(1-p)^2+\left(\nu_{ms}+\frac{5}{4}\right)p(1-p)xS_mS_s+\frac{1}{2}\left(\nu_{ss}+\frac{5}{4}\right)S_s^2p^2x^2-\frac{1-p}{n_m}\ln I_0[\eta_m]-\frac{p}{n_s}\ln I_0[\eta_s]. \tag{3.17}$$

The fraction x of rigid segments on the spacers is determined by minimizing the free energy (2.1) with respect to x: $(\partial F/\partial x)_{S_m,S_s}=0$. From Eqs. (2.9) and (3.17), we obtain

$$(\nu_{ss}+\tfrac{5}{4})pxS_s^2+(\nu_{ms}+\tfrac{5}{4})(1-p)S_mS_s-D(x)=0, \tag{3.18}$$

with

$$D(x)\equiv\ln\left[\frac{x}{(1-x)\lambda}\right]+\frac{1}{tn_s(1-x)}>0, \tag{3.19}$$

and the solution for S_s is given by

$$S_s=\frac{1}{2\left(\nu_{ss}+\frac{5}{4}\right)px}\left\{-\left(\nu_{ms}+\frac{5}{4}\right)(1-p)S_m+\sqrt{\left[\left(\nu_{ms}+\frac{5}{4}\right)(1-p)S_m\right]^2+4\left(\nu_{ss}+\frac{5}{4}\right)pxD(x)}\right\}, \tag{3.20}$$

where λ is defined as

$$\lambda\equiv\left(\frac{e}{z-1}\right)\exp[-\beta f_0]. \tag{3.21}$$

By solving the coupled equations (3.12), (3.13), and (3.20), we can obtain the values of the orientational order parameters S_m, S_s, and the fraction x of rigid segments on the spacers as a function of temperature. From Eq. (3.20) the order parameter S_s is given as a function of S_m and x and so we only solve the coupled equations (3.12) and (3.13) for S_m and x. In the isotropic phase $(S_m=S_s=0)$, the value of x is given by $D(x)=0$:

$$x=\frac{\lambda}{\lambda+\exp[1/tn_s(1-x)]}. \tag{3.22}$$

We further split the local free energy difference f_0 in Eq. (3.21) into two parts:

$$f_0=\epsilon_0-Ts_0, \tag{3.23}$$

where $s_0(=k_B\ln\omega_0)$ is the local entropy loss and $\epsilon_0(<0)$ the energy change needed to straighten a bent bond [15]. The larger values of ϵ_0 correspond to the stiffer spacers. The ω_0 is defined as $\omega_0\equiv\omega_1/\omega_2$ where $\omega_1(\omega_2)$ is the number of states of a straightened (bent) bond. If the segments are placed on a lattice of coordination number z, we have $\omega_0=1/(z-2)$. The stiffness of the spacer is controlled by the ϵ_0. The most flexible spacer chain is realized when $\epsilon_0=0$. Substituting Eq. (3.23) into Eq. (3.21) we obtain

$$\lambda=\omega\exp[-\beta\epsilon_0], \tag{3.24}$$

$\omega\equiv e/[(z-1)(z-2)]$. The free energy per unit segment of our system can be expressed as

$$\beta F/n=\beta h-s/k_B, \tag{3.25}$$

where the entropy s is given by

$$
\begin{aligned}
-s/k_B=p\Big[&-x\ln\omega-\frac{1}{n_s t}\ln(1-x)+(1-x)\ln(1-x)\\
&+x\ln x\Big]+\left(\nu_{mm}+\frac{5}{4}\right)S_m^2(1-p)^2\\
&+2\left(\nu_{ms}+\frac{5}{4}\right)S_mS_s p(1-p)x+\left(\nu_{ss}+\frac{5}{4}\right)S_s^2p^2x^2\\
&-\frac{1-p}{n_m}\ln I_0[\eta_m]-\frac{p}{n_s}\ln I_0[\eta_s], \qquad (3.26)
\end{aligned}
$$

and h is the enthalpy:

$$
\begin{aligned}
\beta h=\beta\epsilon_0 px-\tfrac{1}{2}(\nu_{mm}+\tfrac{5}{4})S_m^2(1-p)^2-(\nu_{ms}+\tfrac{5}{4})S_mS_s p\\
\times(1-p)x-\tfrac{1}{2}(\nu_{ss}+\tfrac{5}{4})S_s^2p^2x^2. \qquad (3.27)
\end{aligned}
$$

When $p=0$, we obtain the free energy for rigid rodlike molecules without spacer chains [38]:

$$\beta F_{\mathrm{nem}}/n_m=\frac{1}{2}\left(\nu_{mm}+\frac{5}{4}\right)S_m^2-\frac{1}{n_m}\ln I_0[\eta_m]. \qquad (3.28)$$

In our numerical calculations, we here define the ratio ξ of the anisotropic interaction as

$$\xi\equiv\nu_{ss}/\nu_{mm}, \qquad (3.29)$$

and assume that the orientational-dependent interaction ν_{ms} between mesogen and spacer segments is proportional to the square root of the product of ν_{mm} and ν_{ss} [39,40]:

$$\nu_{ms}=b\sqrt{\nu_{mm}\nu_{ss}}, \qquad (3.30)$$

where b is the constant. We then obtain

$$\nu_{ss}=\xi\nu_{mm}, \qquad (3.31)$$

$$\nu_{ms}=b\sqrt{\xi}\nu_{mm}. \qquad (3.32)$$

The orientational-dependent interaction parameter ν_{mm} between rigid-mesogen segments is given to be inversely proportional to temperature [13]:

$$\nu_{mm}=U_a/k_BT. \qquad (3.33)$$

IV. NUMERICAL RESULTS AND DISCUSSIONS

In this section we calculate the equilibrium values of the order parameters S_m, S_s, and the fraction x of rigid segments on the spacers as a function of temperature. In the numerical calculations of Sec. III, we here define $\epsilon\equiv|\epsilon_0|/U_a$. The values of ϵ_0 and U_a are of the order of thermal energy. In the following calculations we use $\epsilon=2$, $\omega=0.01$, $b=1$, and $t=100$ for a typical example.

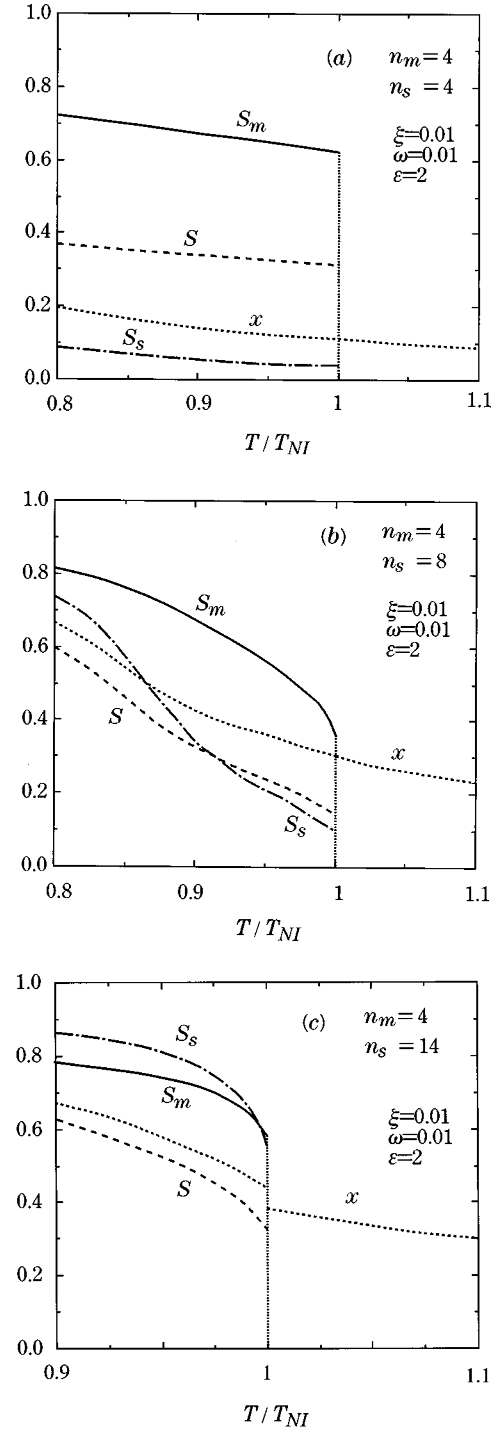

FIG. 2. Order parameters S_m (solid line), S_s (dash-dotted line), the average order parameter S (short-dashed line), and the fraction x (dotted line) of rigid segments on the spacers plotted against the reduced temperature T/T_{NI} with $\xi=0.01$, $n_m=4$, and $t=100$. The number n_s of segments on the spacer is changed from (a) to (c): (a) $n_s=4$; (b) $n_s=8$; (c) $n_s=14$.

Figure 2 shows the order parameters S_m, S_s, S, and the fraction x as a function of the reduced temperature T/T_{NI}, where T_{NI} is the NIT temperature. The curves are calculated with $\xi=0.01$ and $n_m=4$. The number n_s of segments on the spacer is changed from (a) to (c): (a) $n_s=4$; (b) $n_s=8$; (c) $n_s=14$. The solid curve refers to the order parameter S_m of the mesogens and the dash-dotted line shows the order parameter S_s of rigid segments on the spacers. The short-dashed line shows the average-order parameter S and the dotted line corresponds to the fraction x of rigid segments on the spacers. As temperature is decreased, the value of x increases and discontinuously changes at the T_{NI}. For small values of n_s [Fig. 2(a)], the values of x and S_s in the nematic phase are small and the rigid segments on the spacers are

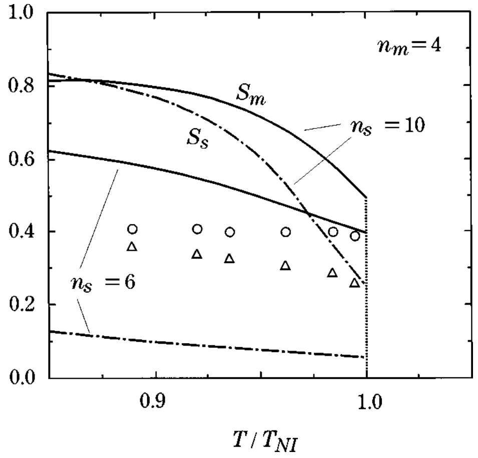

FIG. 3. Comparison of the theoretical calculations with the observed order parameters for polyesters [7].

slightly ordered. The nematic phase is mostly stabilized by the orientational ordering of mesogens. For large values of n_s [Fig. 2(b)], however, the value of x becomes large and the order parameter S_s is sharply increased with decreasing temperature below T_{NI}, where the nematic ordering is enhanced by the ordering of the spacers. As shown in Fig. 2(c), the rigid segments on the long spacers and the mesogens are highly ordered in the nematic phase, where the number of rigid segments on the spacers becomes larger than the axial ratio ($n_m = 4$) of the mesogens. The number of rigid segments on the spacers is given by xn_s. For example, we have $xn_s = 9.3$ at $T/T_{NI} = 0.9$.

Figure 3 shows the comparison of the theoretical calculations with the observed order parameters. The open circles (triangles) show the order parameter of mesogens (spacers) reported for polyesters of 2,2′-dimethyl-4,4′-dihydroxy-azoxybenzene [7]. When $n_s = 6$, the calculated order parameters are mostly independent on temperature and qualitatively describe the experimental data. When the spacer length is large, the calculated order parameters are sharply increased with decreasing temperature.

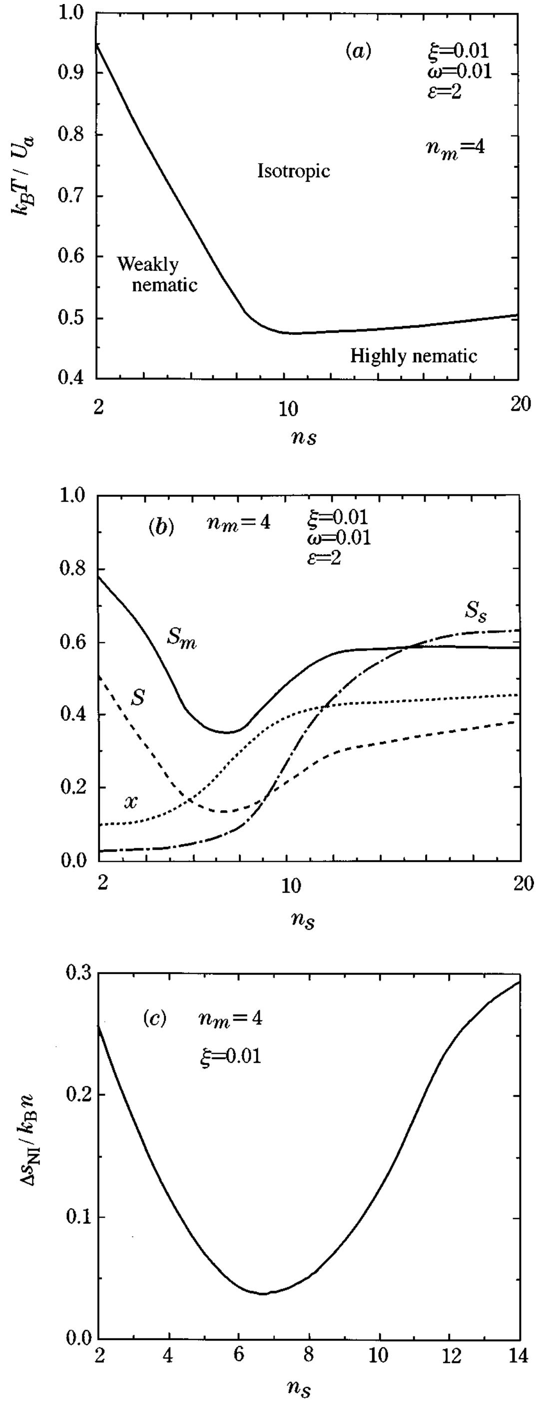

FIG. 4. Dependence on the spacer length of the NIT temperature (a), the order parameters at the NIT point (b), and the entropy change at the NIT point (c) for $\xi = 0.01$.

Figure 4(a) shows the phase diagram on the temperature-spacer length plane for $\xi = 0.01$. The solid line shows the coexistence curve for the isotropic and nematic phases. At small values of n_s, the NIT temperature T_{NI} decreases with increasing the spacer length n_s. At large n_s, however, the T_{NI} slowly increases with increasing n_s. In this region, the spacers increase the degree of nematic ordering in the MLCPs. Figure 4(b) shows the order parameters and the fraction x calculated along the coexistence curve. At small value of n_s, the values of x and S_s along the coexistence curve are small and the rigid segments on the spacers are only slightly ordered at the T_{NI}. The nematic phase is mostly stabilized by the orientational ordering of mesogens. In this sense, the spacer components play a *softening* role. The free energy of the system is minimized by the softening rather than by the ordering of the short spacers. We here call this region a weakly nematic phase. Further increasing the spacer length n_s, the values of the fraction x and the order parameter S_s along the coexistence curve are sharply increased with increasing n_s. The long spacers promote the degree of nematic ordering in the MLCPs and so the NIT temperature T_{NI} slowly increases with increasing n_s. In this sense, the spacers play a *stiffening* role and the nematic ordering of the system is enhanced by the partial ordering of the spacers. We here call this region a highly nematic phase. These two different nematic phases have also been predicted by Vasilenko *et al.* [30]. They predicted the phase transition between the two different nematic phases depending on the fraction of bent bonds on the spacers and the fraction of spacer segments in the repeating unit. As shown in Fig. 4(c), the entropy change $\Delta s_{NI}/(k_B n)$ per unit segment at the NIT point decreases with increasing the spacer length n_s in the weakly nematic phase, or the softening region. However, the entropy

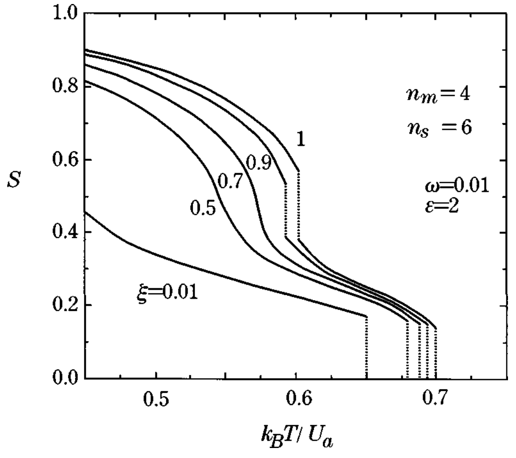

FIG. 5. Dependence on the interaction ratio $\xi \equiv \nu_{ss}/\nu_{mm}$ of the order parameter S with $n_m = 4$ and $n_s = 6$.

change increases with increasing n_s in the highly nematic phase, where the nematic ordering of the spacers gives large contributions to the latent entropy at the T_{NI}. The weakly nematic phase continuously changes to the highly nematic one with increasing spacer length.

Figure 5 shows the dependence on the interaction ratio $\xi \equiv \nu_{ss}/\nu_{mm}$ of the order parameter S with $n_m = 4$ and $n_s = 6$. The value of ξ depends on the chemical structure of the polymer molecules. As the strength of the anisotropic interaction ν_{ss} between the spacers is increased, the NIT temperature and the order parameter increase. Above a critical value of $\xi (= 0.75)$, we find a first-order phase transition between two different nematic phases.

Figure 6 shows the dependence on the temperature of the order parameters and the fraction of rigid segments on the spacers for $\xi = 1$ and $n_m = 4$. The number n_s of segments on the spacer is changed from (a) to (c): (a) $n_s = 4$; (b) $n_s = 6$; (c) $n_s = 12$. As shown in Fig. 6(b), we find a first-order phase transition between two different nematic phases at a critical temperature. At the nematic phase on the high temperature side (weakly nematic phase), the fraction x of rigid segments on the spacers is small and the rigid segments on the spacers are slightly ordered. In the other nematic phase on the low temperature side (highly nematic phase), the rigid segments on the spacers and the mesogens are strongly ordered. Figure 7(a) shows the phase diagram on the temperature-spacer length plane for $\xi = 1$. The solid line shows the isotropic–weakly nematic phase transition, where the NIT temperature T_{NI} decreases with increasing n_s and the spacers play a softening role. The dotted line shows the isotropic–highly nematic phase transition, where the T_{NI} slowly increases with the spacer length and the spacers play a stiffening role. At most combinations of temperature and the spacer length, the equilibrium state of the MLCP is a single uniform phase; isotropic, weakly nematic, highly nematic. These regions are separated by two-phase coexistence curves. We also find the triple point where these three phases coexist. The weakly nematic–highly nematic phase transition line extends from the triple point (TP) to the critical point (CP) at which the properties of the two different nematic phases become indistinguishable and thus the phase transition disappears. This transition line is similar to the gas-liquid phase transition line in the temperature-pressure plane. The dependence of the order parameters along the coexistence curve on the spacer length are shown in Fig. 7(b). On passing through the triple point the order parameters undergo large discrete changes.

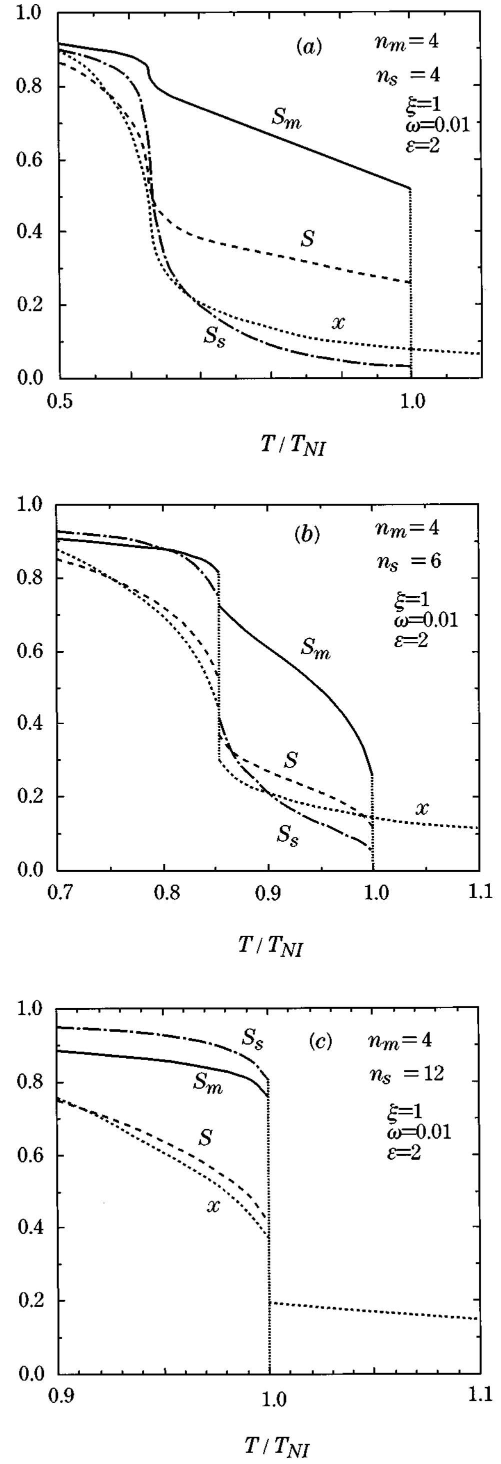

FIG. 6. Dependence on the temperature of the order parameters and the fraction of rigid segments on the spacers for $\xi = 1$. The number n_s of segments on the spacer is changed from (a) to (c): (a) $n_s = 4$; (b) $n_s = 6$; (c) $n_s = 12$.

In Fig. 8, we show the orientational order parameter S plotted against temperature for various values of the energy difference ϵ between the straightened and bent bonds with $n_m = 4$ and $n_s = 10$. The smaller values of ϵ correspond to the more flexible spacers. For large values of ϵ, the order param-

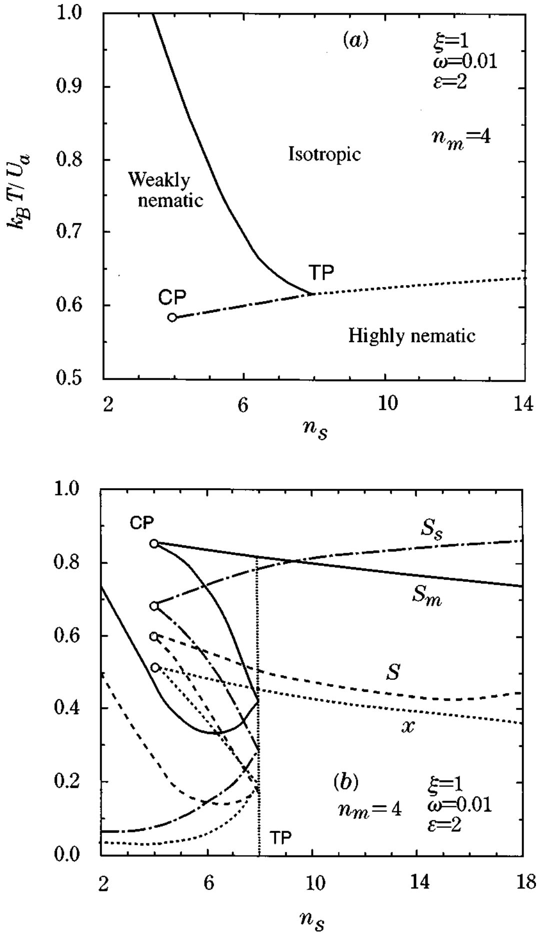

FIG. 7. (a) Phase diagram on the temperature-spacer length n_s plane for $\xi=1$. The solid line shows the isotropic–weakly nematic phase transition and the dotted line shows the isotropic–highly nematic phase transition. The weakly nematic–highly nematic phase transition line extends from the triple point (TP) to the critical point (CP). (b) Order parameters calculated along the coexistence curve.

eter is sharply increased with decreasing temperature due to the nematic ordering not only of mesogens but also of spacers and so the system shows the properties of the highly nematic phase. As the value of ϵ is decreased, the NIT temperature is decreased and the order parameter is slowly increased with decreasing temperature. The system shows the weakly nematic phase. The flexibility of spacers strongly affects the NIT temperature and the nematic ordering.

V. CONCLUSION

We have theoretically studied the nematic-isotropic transitions of MLCPs which consist of rigid mesogens and spacers with various degrees of flexibility. The theory takes into account both the nematic ordering of mesogens and the partial ordering of spacer segments in the nematic phase. We study the nematic ordering of the MLCPs depending on the spacer length, the flexibility of the spacers, and the strength of anisotropic attractive interactions. The main conclusions obtained through this study are as follows.

(1) The theory predicts two different nematic phases. One is a weakly nematic phase, or a softening region, where the fraction of straightened segments on the spacers is small and most spacer chains are only slightly ordered. The weakly nematic phase is mostly formed by the ordering of mesogens. As the result of this, the T_{NI} decreases with increasing the spacer length. The other is a highly nematic phase, or a stiffening region, where the number of straightened segments on the spacers is larger than the axial ratio of mesogens. The straightened segments on the spacers and the mesogens are highly ordered. The ordering of the mesogens is enhanced by the nematic ordering of the spacers. As the result of this, the T_{NI} increases with increasing the spacer length. The MLCPs with sufficiently flexible spacers and the MLCPs with short-semiflexible spacers favor the formation of a weakly nematic phase, while the MLCPs with long-semiflexible spacers promote the formation of a highly nematic phase.

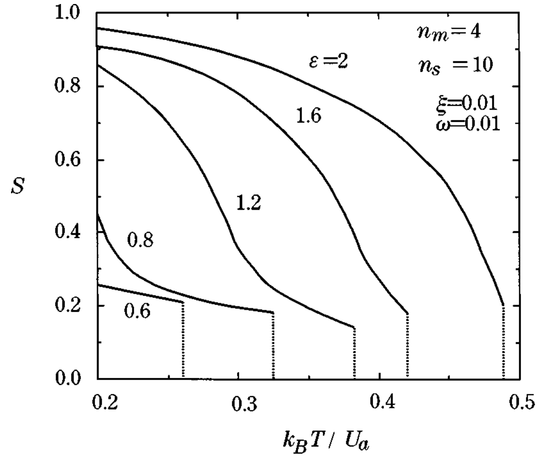

FIG. 8. Orientational order parameter S plotted against temperature for various values of the stiffness parameter ϵ for the spacer with $n_s=10$ and $n_m=4$.

(2) When the anisotropic interaction ratio $\xi \equiv \nu_{ss}/\nu_{mm}$ is small, the isotropic–weakly nematic phase transition line continuously extends to the the isotropic–highly nematic one on the temperature-spacer length plane. When $\xi \approx 1$, however, the first-order phase transition between the two different nematic phases takes place at a critical temperature. In the phase diagram of the temperature-spacer length plane, the isotropic–weakly nematic phase transition line is changed to the isotropic–highly nematic one at the triple point, where the isotropic and two different nematic phases coexist. The weakly nematic–highly nematic phase transition line extends from the triple point to the critical point.

In this paper we focused on the nematic ordering of the MLCPs in melts. The theory will be extended to the phase behaviors of solutions of MLCPs and mixtures of MLCPs with low-molecular-weight liquid crystals.

APPENDIX: LANDAU–DE GENNES EXPANSION

In this appendix, we focus on the vicinity of the NIT point. In order to obtain the approximate formulas of the NIT temperature T_{NI} and the order parameter S, we derive the Landau–de Gennes expansion of our free energy (3.17). We here assume $\nu \equiv \nu_{mm} = \nu_{ms} = \nu_{ss}$ and the value of x is a constant for simplicity. The larger values of x correspond to stiffer spacers. The characteristic ratio l_c of the semiflexible spacers is given by $l_c=(1+x)/(1-x)$ for large n_s [14,35]. Equations (3.6) and (3.8) become

$$\eta_m=n_m(\nu+\tfrac{5}{4})S, \tag{A1}$$

$$\eta_s=n_s x(\nu+\tfrac{5}{4})S, \tag{A2}$$

respectively. Equation (3.11) can be expanded in the η_i as

$$\ln I_0[\eta_i]=\frac{1}{10}\eta_i^2+\frac{1}{105}\eta_i^3-\frac{1}{700}\eta_i^4+\cdots. \tag{A3}$$

Substituting Eq. (A3) into Eq. (3.17), we obtain the nematic free energy as an expansion in the order parameter S:

$$\beta F_{\mathrm{nem}}/n=(\nu+\tfrac{5}{4})(AS^2-BS^3+CS^4), \tag{A4}$$

$$A\equiv\tfrac{1}{2}(1-\tfrac{1}{5}a_1\eta), \tag{A5}$$

$$B\equiv\tfrac{1}{105}a_2\eta^2, \tag{A6}$$

$$C\equiv\tfrac{1}{700}a_3\eta^3, \tag{A7}$$

$$a_1\equiv(1-p)^2+p^2x^2, \tag{A8}$$

$$a_2\equiv(1-p)^3+p^3x^3, \tag{A9}$$

$$a_3\equiv(1-p)^4+p^4x^4, \tag{A10}$$

with

$$\eta\equiv(\nu+\tfrac{5}{4})(n_m+n_s). \tag{A11}$$

The η is given as a function of temperature through the anisotropic interaction ν which is inversely proportional to temperature. The equilibrium value of S is given by minimizing the free energy. The discontinuous phase transition occurs at the NIT point η_{NI},

$$\eta_{NI}=\frac{1}{2}\left(\frac{a_1}{10}+\frac{a_2^2}{63a_3}\right)^{-1}, \tag{A12}$$

where the free energy Eq. (A4) of the isotropic and nematic phases is equal. For $\eta<\eta_{NI}$, we have $S=0$. For $\eta>\eta_{NI}$, the order parameter is given by

$$\begin{aligned}S&=\frac{3B}{8C}\left[1+\sqrt{1-\frac{32AC}{9B^2}}\right]\\&=\frac{5a_2}{2\eta a_3}\left[1+\sqrt{1+\frac{28a_1a_3}{5a_2^2}\left(1-\frac{5}{a_1\eta}\right)}\right].\end{aligned} \tag{A13}$$

The order parameter S_{NI} at the NIT point is given by

$$S_{NI}=\frac{B}{2C}=\frac{20a_2}{3a_3}\left(\frac{a_1}{10}+\frac{a_2^2}{63a_3}\right). \tag{A14}$$

The order parameter S starts at S_{NI} and gradually approaches 1 with increasing η (or decreasing temperature). From Eqs. (A11) and (A12), the NIT temperature is given by

$$T_{NI}=\frac{U_a}{k_B}\left(\frac{1-p}{n_m}\eta_{NI}-\frac{5}{4}\right)^{-1}. \tag{A15}$$

For $T<T_{NI}$, the nematic phase becomes stable. For sufficiently flexible spacers $(x=0)$, the NIT temperature T_{NI} decreases with increasing the spacer length n_s, where the spacers play a softening role. For stiffer spacers, or larger values of x, the temperature T_{NI} has a minimum as a function of the spacer length. At large values of n_s, the temperature T_{NI} increases with increasing n_s, where the spacers play a stiffening role.

We here derive the approximate formulas for the NIT temperature and the order parameter at the T_{NI} for the following three cases. For MLCPs with sufficiently flexible spacers, we can set $x=0$ and so we obtain $a_1=(1-p)^2$, $a_2=(1-p)^3$, and $a_3=(1-p)^4$. From Eq. (A15), the NIT temperature is given by

$$T_{NI}=\frac{4(U_a/k_B)(1-p)}{5[p-(1-3.45/n_m)]}. \tag{A16}$$

The NIT temperature is decreased with increasing the fraction p of spacer segments at $p>1-3.45/n_m$. This tendency agrees with the experimental results of a homologous series of thermotropic polyesters based on 4,4′-dihydroxy-2,2′-dimethylazoxybenzene and various alkanedioic acid [7], where the NIT temperature is decreased as the number of methylene groups in the spacer increases. The experimental data show an odd-even effect, however, we neglect the parity effects [41,42] in this paper. The order parameter S_{NI} at the NIT point is decreased with increasing p as

$$S_{NI}=0.772(1-p). \tag{A17}$$

For rigid rods without spacer chains, we can set $p=0$ and $a_1=a_2=a_3=1$. The value of η at the NIT point is $\eta_{NI}=315/73$ and so we obtain

$$T_{NI}=\frac{4(U_a/k_B)n_m}{5(3.45-n_m)}, \tag{A18}$$

and $S_{NI}=0.772$. The T_{NI} increases with increasing n_m and diverges at $n_m=3.45$. When the axial ratio n_m of the mesogens is larger than 3.45, the nematic phase is stable at all temperatures. For larger values of n_m, the repulsive interaction between rigid rods dominates and the attractive interaction plays only an auxiliary role in the NIT and so the T_{NI} diverges [17,23,38].

When $p=1$, we can obtain the formula for semiflexible polymers without mesogen segments [35]. The stiffness of the polymer is controlled by $x\equiv n_r/n_s$. From Eq. (A15), we obtain

$$T_{NI}=\frac{4(U_a/k_B)n_s}{5(3.45/x^2-n_s)}, \tag{A19}$$

and $S_{NI}=0.772x$. The temperature T_{NI} is increased with increasing n_s at $n_s<3.45/x^2$. For long-semiflexible chains $(x\ll 1)$, the order parameter at the NIT point is small and the transition becomes mostly second order. This result qualitatively agrees with the properties of the NIT for the elastic wormlike chain [24].

[1] *Liquid Crystalline and Mesomorphic Polymers*, edited by V. P. Shibaev and L. Lam (Springer-Verlag, New York, 1993).

[2] *Liquid Crystalline Polymers*, edited by R. A. Weiss and C. K. Ober (American Chemical Society, Washington, D.C., 1990).

[3] W. Brostow, Polymer **31**, 979 (1990).

[4] A. Blumstein and O. Thomas, Macromolecules **15**, 1264 (1982).

[5] A. F. Martins, J. B. Ferreira, F. Volino, A. Blumstein, and R. B. Blumstein, Macromolecules **16**, 279 (1983).

[6] G. Sigaud, D. Y. Yoon, and A. C. Griffin, Macromolecules **16**, 875 (1983).

[7] E. T. Samulski, M. M. Gauthier, R. B. Blumstein, and A. Blumstein, Macromolecules **17**, 479 (1984).

[8] J. F. D'Allest, P. Maissa, A. ten Bosch, P. Sixou, A. Blumstein, R. Blumstein, J. Teixeira, and L. Noirez, Phys. Rev. Lett. **28**, 2562 (1988); Mol. Cryst. Liq. Cryst. **155**, 581 (1988).

[9] V. Arrighi, J. S. Higgins, L. Abis, and W. A. Weiss, Polymer **37**, 141 (1996).

[10] P. Cavalleri, A. Cifferri, C. DellErba, M. Vovi, and B. Purevsuren, Macromolecules **30**, 3513 (1997).

[11] L. Onsager, Ann. (N.Y.) Acad. Sci. **51**, 626 (1949).

[12] W. Maier and A. Saupe, Z. Naturforsch. A **14a**, 882 (1959).

[13] P. G. de Gennes and J. Prost, *The Physics of Liquid Crystals*, 2nd ed. (Oxford Science, London, 1993).

[14] P. J. Flory, Proc. R. Soc. London, Ser. A **234**, 60 (1956).

[15] P. J. Flory, Proc. R. Soc. London, Ser. A **234**, 73 (1956).

[16] P. J. Flory, Macromolecules **11**, 1141 (1978).

[17] P. J. Flory and G. Ronca, Mol. Cryst. Liq. Cryst. **54**, 289 (1979); **54**, 311 (1979).

[18] M. Warner and P. J. Flory, J. Chem. Phys. **73**, 6327 (1980).

[19] R. R. Matheson and P. J. Flory, Macromolecules **14**, 954 (1981).

[20] N. Saito, K. Takahashi, and Y. Yunoki, J. Phys. Soc. Jpn. **22**, 219 (1967).

[21] K. F. Freed, Adv. Chem. Phys. **22**, 1 (1972).

[22] F. Jahnig, J. Chem. Phys. **70**, 3279 (1979).

[23] G. Ronca and D. Y. Yoon, J. Chem. Phys. **76**, 3295 (1982).

[24] A. ten Bosch, P. Maissa, and P. Sixou, J. Chem. Phys. **79**, 3462 (1983); J. Phys. (France) Lett. **44**, L105 (1983).

[25] M. Warner, J. M. F. Gunn, and A. Baumgartner, J. Phys. A **18**, 3007 (1985); X. J. Wang and M. Warner, *ibid.* **19**, 2215 (1986).

[26] J. B. Lagowski and J. Noolandi, Mol. Cryst. Liq. Cryst. **198**, 371 (1991).

[27] Z. Y. Chen, Macromolecules **26**, 3419 (1993); Phys. Rev. E **47**, 3765 (1993).

[28] A. R. Khokhlov, Phys. Lett. **68A**, 135 (1978); A. Y. Grosberg and A. R. Khokhlov, Adv. Polym. Sci. **41**, 53 (1981).

[29] A. R. Khokhlov and A. N. Semenov, J. Stat. Phys. **38**, 161 (1985); Physica A **108**, 546 (1981); **112**, 605 (1985).

[30] S. V. Vasilenko, A. R. Khokhlov, and V. P. Shibaev, Macromolecules **17**, 2270 (1984).

[31] G. H. Fredrickson and L. Leibler, Macromolecules **23**, 531 (1990).

[32] X. J. Wang and M. Warner, Liq. Cryst. **12**, 385 (1992).

[33] H. Kimura, in *Liquid Crystals for Advanced Technologies*, edited by T. J. Bunning *et al.*, MRS Symposia Proceedings No. 425 (Materials Research Society, Pittsburgh, 1996), p. 113.

[34] R. Holyst and T. A. Vilgis, Macromol. Theory Simul. **5**, 573 (1996).

[35] A. Matsuyama, Y. Sumikawa, and T. Kato, J. Chem. Phys. **107**, 4711 (1997).

[36] G. Ronca and D. Y. Yoon, J. Chem. Phys. **83**, 373 (1985).

[37] P. J. Flory, *Principles of Polymer Chemistry* (Cornell University, Ithaca, 1953).

[38] A. Matsuyama and T. Kato, J. Chem. Phys. **105**, 1654 (1996); A. Matsuyama, R. Morii, and T. Kato, Mol. Cryst. Liq. Cryst. (to be published).

[39] P. G. de Gennes, *Scaling Concepts in Polymer Physics* (Cornell University, Ithaca, 1979).

[40] H. W. Chiu, Z. L. Zhou, T. Kyu, L. G. Cada, and L. C. Chien, Macromolecules **29**, 1051 (1996).

[41] S. Marcelja, J. Chem. Phys. **60**, 3599 (1974).

[42] H. S. Serpi and D. J. Photinos, J. Chem. Phys. **105**, 1718 (1996).